Inorganic Chemistry

Article

pubs.acs.org/IC

$\{Sn_9[Si(SiMe_3)_3]_2\}^{2-}$: A Metalloid Tin Cluster Compound With a Sn_9 Core of Oxidation State Zero†

Claudio Schrenk,‡ Florian Winter,§ Rainer Pöttgen,§ and Andreas Schnepf*,‡

‡Chemistry Department, University Duisburg-Essen, Universitätsstrasse 5-7, D-45117 Essen, Germany

§Institut für Anorganische und Analytische Chemie, Universität Münster, Corrensstrasse 30, D-48149 Münster, Germany

Supporting Information

ABSTRACT: The disproportionation reaction of the subvalent metastable halide SnCl proved to be a powerful synthetic method for the synthesis of metalloid cluster compounds of tin. Now we present the synthesis and structural characterization of the anionic metalloid cluster compound $[Sn_9[Si(SiMe_3)_3]_2]^{2-}$ **3** where the oxidation state of the tin atoms is zero. Quantum chemical calculations as well as Mössbauer spectroscopic investigations show that three different kinds of tin atoms are present within the cluster core. Compound **3** is highly reactive as shown by NMR investigations, thus being a good starting material for further ongoing research on the reactivity of such partly shielded metalloid cluster compounds.

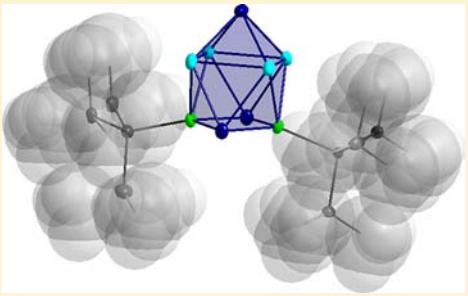

INTRODUCTION

Polyhedral cluster compounds of the heavier elements of group 14 have attracted much interest in recent years as these compounds might give insight into the area between molecules and the solid state on a molecular level,[1] being thus also of central interest for nanotechnology. For the synthesis of ligand stabilized clusters of group 14, different synthetic routes have been identified.[2] One synthetic route applies the disproportionation reaction of a metastable subhalide while another one applies reductive coupling reactions, where ligand stripping can lead to naked, ligand free tetrel atoms pushing the average oxidation state of the tetrel atoms to the value zero of the solid state.[3] Another synthetic route starts from polyhedral Zintl anions,[1] and recently, it was shown that also clusters with a positive oxidation state of the tetrel atoms are available from Zintl anions, where the average oxidation state of the tetrel atoms is negative. Hence the reaction of Ge_9^{4-} with Cl–$Si(SiMe_3)_3$ gives $\{Ge_9[Si(SiMe_3)_3]_3\}^-$ **1**,[4] which is also available from the reaction of GeBr with $LiSi(SiMe_3)_3$,[5] showing a direct correlation between metalloid clusters and substituted Zintl anions.

Interestingly, in the area of polyhedral group 14 clusters, besides a variety of ligand stabilized germanium clusters of composition $Ge_9R_2^{2-}$ [R = Ph_2Bi;[6] Ph/$SbPh_2$;[7] Ph_3Sn/Ph_3Ge;[8] CH═CH—Fc (Fc = ferrocenyl);[9] C_2H_3/CH_2–$CH(CH_2)_2$[10]], which are available from the Zintl anion Ge_9^{4-}, no $Sn_9R_2^{2-}$ compound could be isolated so far. However, Sn_9R^{3-} clusters with one substituent have already been structurally characterized,[11,12] and mass spectroscopic investigations hint to the presence of $Sn_9R_2^{2-}$ species in solution.[12] We now present the first structurally characterized $Sn_9R_2^{2-}$ cluster, which could be synthesized applying the disproportionation reaction of a Sn(I) halide solution.

RESULT AND DISCUSSION

Recently, we could show that metalloid tin clusters can be obtained by the reaction of a Sn(I) halide solution using $LiSi(SiMe_3)_3$ as a metathesis reagent.[13] Thereby it becomes obvious that the product (the metalloid cluster) obtained strongly depends on the subvalent halide source applied (Scheme 1). The subvalent halide source is thereby obtained by a preparative cocondensation technique[14] which leads to a Sn(I) halide emulsion when NBu_3 is used as a donor molecule while an isolable solution is obtained when the donor PBu_3 is used.[15] In both cases the solvent is toluene. Applying now the emulsion as the subhalide source in the reaction with $LiSi(SiMe_3)_3$, the neutral metalloid cluster $Sn_{10}[Si(SiMe_3)_3]_6$ **1** is obtained.[16] Besides this, using the isolable solution the anionic metalloid cluster $\{Sn_{10}[Si(SiMe_3)_3]_5\}^-$ **2** is obtained.[15] Hence, the product of the reaction strongly depends on the reactivity of the subhalide and thereby on the donor applied.[17]

Another important factor which can be manipulated and which might influence the reactivity of the subhalide source is the Sn/halide ratio within the subhalide solution, being normally in the range between 1.1 and 1.2, i.e., the ratio of Sn(I)X with respect to Sn(II)X_2 (X = halide like Cl, Br) varies between 90:10 and 80:20. The Sn/halide ratio is thereby adjusted by the temperature of the reactor during the synthesis of the high temperature molecule SnX, i.e., the lower the temperature the higher the Sn(II) halide ratio.[14] In the case of the synthesis of the metalloid cluster **2**, a SnCl solution with a Sn/Cl ratio of ca. 1.1 was used. When the reaction is now performed applying a SnCl solution with a Sn:Cl ratio of 1.2, where the amount of Sn(II)Cl_2 is significantly higher, a different behavior is observed; i.e., during workup we were not

Received: June 1, 2012
Published: July 17, 2012

   dx.doi.org/10.1021/ic3011647 | Inorg. Chem. 2012, 51, 8583–8588

Scheme 1. Schematic Presentation of the Synthesis of Metalloid Sn-Clusters Applying Various Sn(I) Halide Precursors (Emulsion or Solution) Depending on the Donor Applied During the Cocondensation Reaction

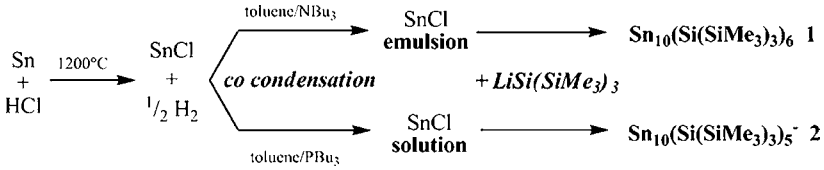

able to isolate **2** or **1**.[18] However, mass spectra of the crude reaction mixture clearly show that anionic clusters are formed during the reaction.[19] As the reaction is performed within toluene as solvent it is unlikely that separated ions are present within the solution, which should be insoluble and precipitate. Consequently, contact ion pairs should be present within the solution; i.e., to precipitate an ionic product we added tetramethylethylendiamine (TMEDA) as a complexing reagent for the lithium cations to the reaction solution and obtained first of all black, blocklike crystals, whose crystal structure could not be solved so far, due to severe crystallographic problems.[20] However, on concentrating the filtrated solution another compound is obtained in the form of dark- red needlelike crystals. Crystal structure solution of these crystals shows that the metalloid cluster compound $\{Sn_9[Si(SiMe_3)_3]_2\}^{2-}$ **3** has formed, which crystallizes together with two $[Li(TMEDA)_2]^+$ cations in the orthorhombic space group *Pnma*. The molecular structure of **3** is shown in Figure 1 and is best described as a

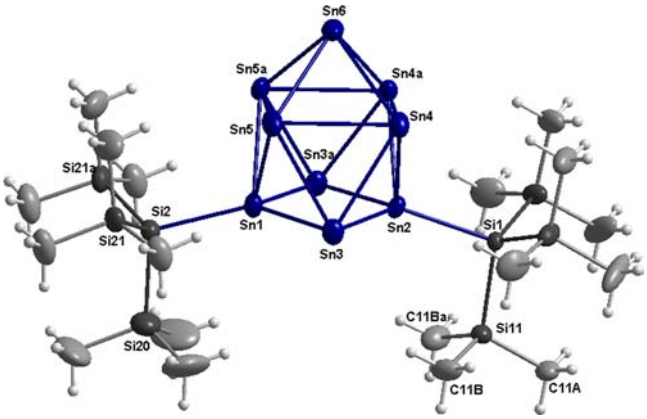

Figure 1. Molecular structure of $\{Sn_9[Si(SiMe_3)_3]_2\}^{2-}$ **3**. Displacement ellipsoids are shown at the 50% probability level. Selected bond distances (pm) and angles (deg): Sn1−Sn3 289.09(7), Sn3−Sn2 289.50(7), Sn1−Sn5 298.58(9), Sn2−Sn4 296.29(9), Sn4−Sn4a 321.97, Sn5−Sn5a 325.07, Sn4−Sn5 310.91(8), Sn4−Sn6 295.73(10), Sn5−Sn6 295.33(10), Sn1−Si2 258.0(3), Sn2−Si1 257.9(3), Si1−Si11 234.3(4), Si2−Si20 234.7(5), Si2−Si21 233.4(3), Si11−C11A 187.0(12), Si11−C11B 187.3(10), Sn1−Sn3−Sn2 74.17(2), Sn3−Sn1−Sn3a 105.92(3), Sn4−Sn3−Sn5 61.41(2), Sn5−Sn4−Sn4a 90.29(2), Sn5−Sn1−Si2 106.71(7), Si1−Si11−C11A 112.5, Si1−Si11−C11B 109.0(3).

monocapped square antiprismatic arrangement of nine tin atoms, where two tin atoms in the noncapped rectangle (Sn1 and Sn2) are bound to one ligand each. Compound **3** is thus the first example of an $E_9R_2^{2-}$ cluster in tin chemistry which is obtained via the disproportionation reaction of a tin subhalide. The oxidation state of the tin atoms within the cluster core is zero as is the case for the isostructural germanium clusters $Ge_9R_2^{2-}$ [6−10] obtained from a reaction of Ge_9^{4-}. Consequently, **3** is another example of a direct connection of the two different synthetic routes starting from Zintl anions or monohalide solutions. The Sn_9 polyhedron within **3** is comparable to the Ge_9 polyhedron found within $Ge_9R_2^{2-}$ clusters, however, exhibiting longer E−E distances due to the larger covalent radius of tin with respect to germanium.[21] The capped Sn_4 square (Sn4, Sn5, Sn4a, Sn5a) is thereby distorted to a rectangle in which the longest Sn−Sn distances of 325.07 pm (Sn5−Sn5a) and 310.91 pm (Sn4−Sn5) are found. Besides this, within the noncapped Sn_4 square (Sn1, Sn3, Sn2, Sn3a) the Sn−Sn distances are in a narrow range (289.1−289.5 pm), exhibiting a dihedral angle of 1.5°. However, a diamond arrangement is realized as diagonal distances of 349 pm (Sn1−Sn2) and 462 pm (Sn3−Sn3a) are found. All other tin−tin distances within the cluster core vary in a small range between 289.09 pm (Sn1−Sn3) and 306.15 pm (Sn3−Sn6). The arrangement of the nine tin atoms within the cluster core might also be described as a tricapped trigonal prismatic arrangement, where two ligand bound tin atoms (Sn1, Sn2) bear a ligand and the third one (Sn6) is naked.

However, the trigonal prism is strongly distorted as the heights of the prism differ by more than 100 pm (Sn3−Sn3a 462 pm, Sn4−Sn4a 322 pm, Sn5−Sn5a 325 pm). Nevertheless, the tin−tin distances to the capping tin atoms are very similar as the ligand bound tin atoms show average tin−tin distances of 293.4 pm (289.1−298.6) while the naked capping tin atom (Sn6) is bound to the cluster core with average tin tin distances of 295.5 pm (295.3−295.7), being thereby the naked tin atom with the shortest tin−tin contacts within the cluster core. Hence, the capping tin atom (Sn6) exhibits an emersed position, and is also easily available for further reactions as to be seen from the space filling model in Figure 2.

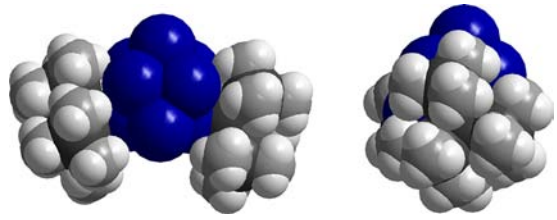

Figure 2. Space filling model of $\{Sn_9[Si(SiMe_3)_3]_2\}^{2-}$ **3**; view along two perpendicular directions.

As discussed before the arrangement of the nine tin atoms within the cluster core of **3** can be described as being between a *closo* (tricapped trigonal prism) and a *nido* (monocapped square antiprism) structure as it is frequently observed in group 14 E_9 cluster compounds.[22] Additionally, quantum chemical calculations[23] on the model compound $Sn_9H_2^{2-}$, for which a similar structure as found in **3** is calculated, show significant leaps in the orbital energy between HOMO − 9 and HOMO − 11, indicating the presence of 20−22 skeletal electrons, being thus in line with Wade's rules,[24] where $2n + 4$ $(2n + 2)$ bonding

dx.doi.org/10.1021/ic3011647 | *Inorg. Chem.* 2012, 51, 8583−8588

electrons are expected for a *nido* (*closo*) cluster compound like **3** (n = 9). Further calculations on **3** show that the nine tin atoms within the cluster core of **3** can be divided into three different groups of tin atoms with respect to their calculated charge based on occupation numbers; i.e., tin atoms with average charges of −0.35, −0.12 and +0.16 are present (Figure 3).[25] The presence of three different kinds of tin atoms as

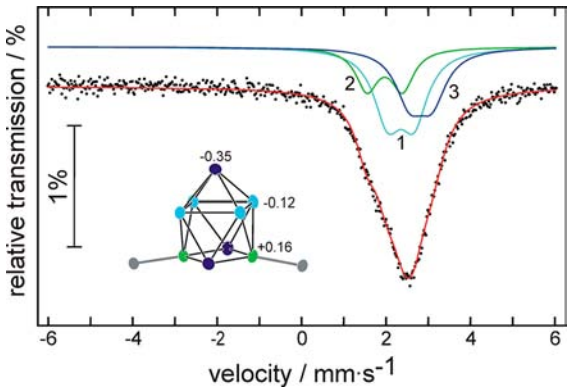

Figure 3. Experimental and simulated ^{119}Sn Mössbauer spectrum of $\{Sn_9[Si(SiMe_3)_3]_2\}\{Li(TMEDA)_2\}_2$ at 78 K. The subspectra of the tin species 1, 2, and 3 are drawn in blue, green, and violet, similar to the tin cluster. The calculated charges of the three sets of tin atoms are indicated.

indicated by the calculations is corroborated experimentally by ^{119}Sn Mössbauer spectroscopy. The ^{119}Sn Mössbauer spectrum of $\{Sn_9[Si(SiMe_3)_3]_2\}\{Li(TMEDA)_2\}_2$ recorded at 78 K is presented in Figure 3 together with a transmission integral fit. The corresponding fitting parameters are listed in Table 1.

Table 1. Fitting Parameters of a ^{119}Sn Mössbauer Spectroscopic Measurement for $\{Sn_9[Si(SiMe_3)_3]_2\}\{Li(TMEDA)_2\}_2$ at 78 K[a]

site	δ/mm s^{-1}	ΔE_Q/mm s^{-1}	Γ/mm s^{-1}
Sn1 (blue)	2.35(2)	0.63(4)	0.79(2)
Sn2 (green)	1.97(3)	0.84(7)	0.64(2)
Sn3 (violet)	2.82(5)	0.5(1)	0.81(3)

[a]Numbers in parentheses represent the statistical errors in the last digit. δ, isomer shift; ΔE_Q, electric quadrupole splitting; Γ, experimental line width. The intensities of Sn1:Sn2:Sn3 were fixed at 4:2:3.

A reasonable fit of the spectrum was possible with three superimposed subspectra which are all subjected to quadrupole splitting. The correct assignment of these sites was possible via the calculated partial charges. The population analyses (*vide supra*) revealed three groups of tin atoms with charges of −0.35, −0.12, and +0.16 in 3:4:2 ratio. A higher negative charge is in line with a higher electron density at the tin nucleus and thus with a higher isomer shift.[26] When constraining the signal areas in the above ratio we got a good reproduction of the experimental spectrum. The highest quadrupole splitting parameter is observed for the Sn2 atoms which are connected to the ligands.

Due to the quantum chemical calculations as well as ^{119}Sn Mössbauer experiments, three different kinds of tin atoms are presents within **3**, where three (Sn3, Sn3a, Sn6) of the nine tin atoms exhibit a comparably high negative charge, being thus the most reactive place for subsequent reactions applying electrophiles. However, only the capping tin atom (Sn6) is easily available (Figure 2). Additionally, HOMO − 4 (Figure 4) is localized at the open side of **3** exhibiting a high lone-pair character at Sn6, being perfectly oriented for further reactions.

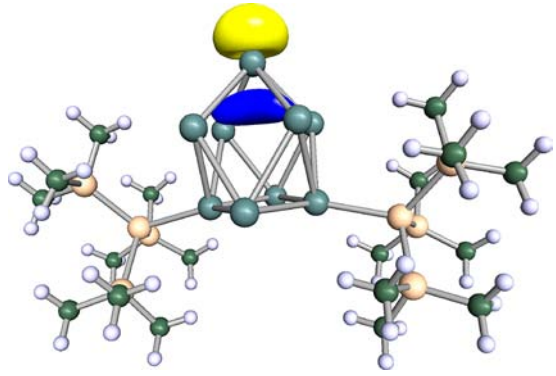

Figure 4. Representation of HOMO − 4 of $\{Sn_9[Si(SiMe_3)_3]_2\}^{2-}$ **3**.

Consequently, **3** is a perfect starting material for further investigations on the reactivity of such a polyhedral tin cluster compound (vide infra).[27] However, to perform further reactions **3** has to be dissolved first. Thereby, **3** is easily dissolved in tetrahydrofuran (THF), leading to a dark red, nearly black solution. However, proton NMR measurements of the THF solution of **3**·$[Li(TMEDA)_2]_2$ unambiguously show not only that **3**·$[Li(TMEDA)_2]_2$ is dissolved in THF but also that subsequent reactions take place as we find a time dependency of the spectra.[28] These subsequent reactions lead at the end to a black precipitate of unknown composition,[29] while a colorless solution is obtained. Mass spectroscopic investigations of a THF solution of **3**·$[Li(TMEDA)_2]_2$ also hint to a dynamic system in solution, as we see besides cluster compounds exhibiting nine tin atoms also compounds exhibiting 10 tin atoms, e.g., $\{Sn_{10}[Si(SiMe_3)_3]_3\}^-$ (m/z = 1940), which can be identified by its isotopic pattern (Figure 5). Additionally, the signal with the highest intensity at m/z = 1820 au is not the monoanionic compound $\{Sn_9[Si(SiMe_3)_3]_2\}^-$ but the monoanionic compound $\{Sn_9[Si(SiMe_3)_3]_3\}^-$ **4**,[30] which is also clearly identified by its isotopic pattern. Hence, a complex reaction cascade is taking place on dissolving crystals of **3**·$[Li(TMEDA)_2]_2$ in THF as indicated by NMR and mass spectroscopy.

Sadly, **3**·$[Li(TMEDA)_2]_2$ is insoluble in, e.g., toluene, and the reaction pathway of the decomposition reaction is unclear up to now. Nevertheless, we assumed that the countercation might play an important role during the decomposition, and thus, we added a stronger complexing reagent to the solution.

The addition of 12-crown-4 thereby leads to a THF solution of **3** with enhanced stability as can be seen in the proton NMR spectra, where we now observe the signal of **3** for a longer period of time (Figure 6); i.e., the degradation of **3** is now taking place within a couple of days and not minutes, maybe being enough for subsequent reactions.

As a proof of principle reaction we added Cl−$Si(SiMe_3)_3$ to the THF solution of **3**, exhibiting 12-crown-4, leading to a stable reaction solution with a white precipitate of LiCl. Workup of the reaction mixture leads to the anticipated compound $\{Sn_9[Si(SiMe_3)_3]_3\}^-$ **4** in 60% isolated yield, showing that **3** can be used as a starting material for a variety

dx.doi.org/10.1021/ic3011647 | *Inorg. Chem.* 2012, 51, 8583−8588

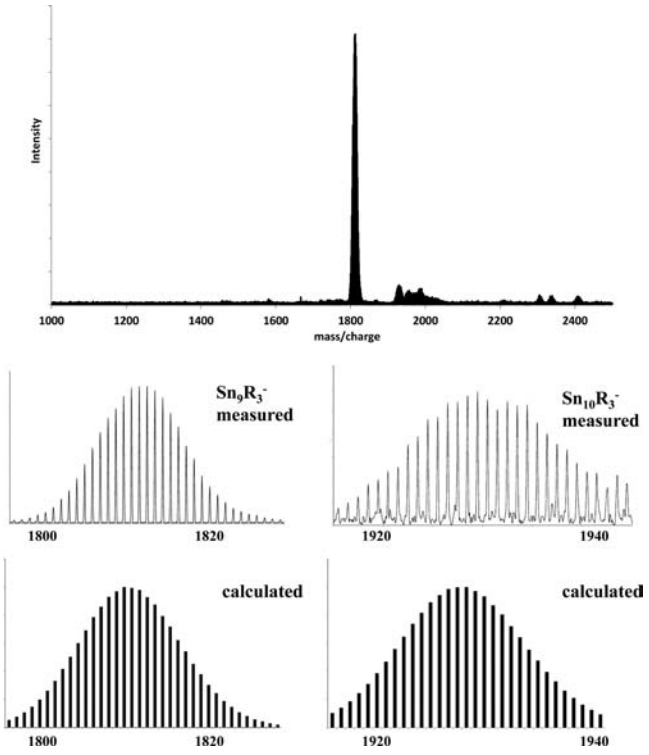

Figure 5. Top: Mass spectra of a THF solution of dissolved crystals of **3**·$[Li(TMEDA)_2]_2$ applying electrospray ionization. Bottom: Calculated and measured isotopic pattern of $Sn_9R_3^-$ **4** (left) and $Sn_{10}R_3^-$ (right); R = $Si(SiMe_3)_3$.

of further reactions. Thereby a second reaction applying Cl-$SiMe_3$ did not lead to a stable compound, which can be seen from a tin mirror that formed on the walls of the flask during the reaction. Hence, the possible product $\{Sn_9[Si(SiMe_3)_3]_2SiMe_3\}^-$ **5** seems to be unstable and decomposes among others to elemental tin. The highly dynamic behavior of **3** might be due to weak tin−tin bonds within the cluster core. This property of **3** is first of all negative due to the challenging handling but might be also a chance for further build up reactions on the way to larger clusters with more than nine tin atoms.

In summary, we presented the synthesis and structural characterization as well as Mössbauer and NMR spectroscopic investigations of $\{Sn_9[Si(SiMe_3)_3]_2\}^{2-}$ **3**, being the first structurally characterized tin cluster, where the tin atoms exhibit the oxidation state zero. Compound **3** can be dissolved in THF leading to a highly dynamic system in solution which can be altered by complexing the countercation with 12-crown-4. Thereby the reaction of **3** with Cl−$Si(SiMe_3)_3$ leads to $\{Sn_9[Si(SiMe_3)_3]_3\}^-$ **4** in good yield showing that **3** can be used as a starting material for further ongoing build-up reactions.

EXPERIMENTAL SECTION

Synthesis of $\{Sn_9[Si(SiMe_3)_3]_2\}$ (3)·$[Li(TMEDA)_2]_2$. A metastable Sn(I)Cl solution was prepared by using a cocondensation technique, where 3.95 g (33.2 mmol) of tin reacted with 40 mmol of HCl at 1240 °C and the resulting gaseous Sn(I)Cl was condensed at −196 °C with a mixture of toluene and P(*n*-Bu)$_3$ (volume ratio 10:1). After warming up to −78 °C, a dark red solution is obtained. A 20 mL portion of this solution (4 mmol SnCl) is added to 2.1 mg (4.4 mmol) of $LiSi(SiMe_3)_3$·3THF at −78 °C. The reaction mixture was slowly warmed up to room temperature, and a black reaction solution is obtained. To this solution is added 2 mL (12 mmol) of tetramethylethylene-diamine (TMEDA) leading to black crystals of so far unknown composition (200 mg). The crystals are separated, and the mother solution is concentrated in vacuo. After the addition of 1 mL (6 mmol) of TMEDA the solution is stored at room temperature for 24 h, leading to dark red crystals of $\{Sn_9[Si(SiMe_3)_3]_2\}$·$[Li(TMEDA)_2]_2$ (100 mg, 0.05 mmol, 11%).

NMR Spectroscopy.

(a) A couple of crystals of $\{Sn_9[Si(SiMe_3)_3]_2\}$·$[Li(TMEDA)_2]_2$ are placed within an NMR tube. After the addition of 0.6 mL of THF-d_8, the solution is freezed with liquid nitrogen and the NMR tube is flame-sealed under vacuum. After melting of the solution the NMR tube is directly put in the NMR spectrometer, and proton NMR spectra are measured every 15 min.

(b) A couple of crystals of $\{Sn_9[Si(SiMe_3)_3]_2\}$·$[Li(TMEDA)_2]_2$ are placed within an NMR tube. After the addition of 0.6 mL of THF-d_8 and 0.1 mL of 12-crown-4, the resulting solution is frozen with liquid nitrogen, and the NMR tube is flame-sealed under vacuum. After melting of the solution the NMR tube is directly put in the NMR spectrometer, and proton NMR spectra are measured every day.

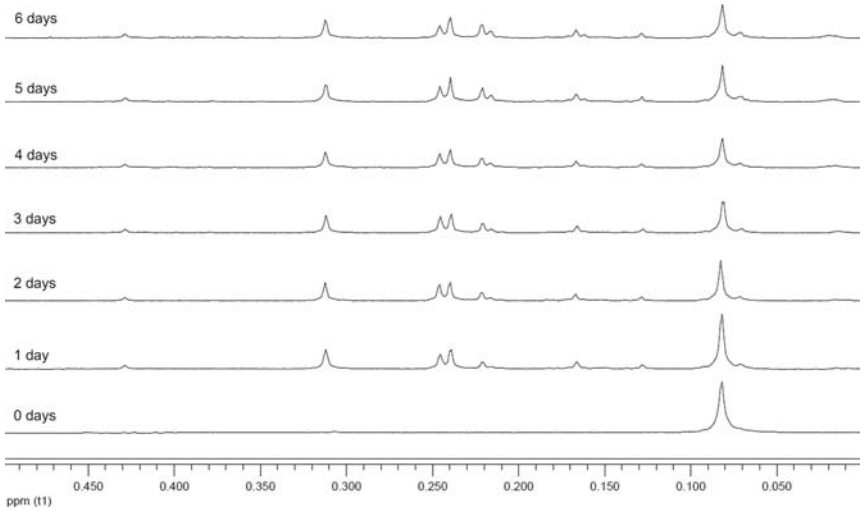

Figure 6. Time dependency of the proton NMR spectra of a THF solution of **3**·$[Li(TMEDA)_2]_2$ stabilized by 12-crown-4.

dx.doi.org/10.1021/ic3011647 | *Inorg. Chem.* 2012, 51, 8583−8588

^{1}H NMR (THF-d_8): 0.08 (s, 54 H, SiMe_3), 3.63 (s, 64 H, O−CH_2). The measurement of ^{13}C and ^{29}Si NMR spectra was not possible due to the poor stability of compound **3**.

Mass Spectrometry. The anionic cluster compounds were brought into the gas phase by electrospraying[31] a THF solution of dissolved crystals of $\{Sn_9[Si(SiMe_3)_3]_2\}\cdot[Li(TMEDA)_2]_2$. The endplate of the electrospray source was typically held at a potential of +3.2 kV relative to the electrospray needle which was grounded. A potential of +3.3 kV was applied to the entrance of the metal coated quartz capillary.

^{119}Sn Mössbauer Spectroscopy. A $Ca^{119m}SnO_3$ source was used for the ^{119}Sn Mössbauer spectroscopic investigation. The sample was placed within a thin-walled glass container at a thickness of about 10 mg Sn/cm^2. A palladium foil of 0.05 mm thickness was used to reduce the tin K X-rays concurrently emitted by this source. The measurement was conducted in the usual transmission geometry at 78 K with a total counting time of one day.

X-ray Crystallography. Table 2 contains the crystal data and details of the X-ray structural determination for $\{Sn_9[Si(SiMe_3)_3]_2\}\cdot[Li(TMEDA)_2]_2$ and $\{Sn_9[Si(SiMe_3)_3]_2\}\cdot[Li(THF)_4]_2\cdot3THF$. The data were collected at 150 K on a Bruker APEX II (**3**·$[Li(TMEDA)_2]_2$) or a STOE IPDS II (**3**·$[Li(THF)_4]_2$·3THF) diffractometer employing monochromated Mo Kα (λ = 0.710 73 Å) radiation from a sealed tube and equipped with an Oxford Cryosystems cryostat. The structure was solved by direct methods and refined by full-matrix least-squares techniques (programs used: SHELXS and SHELXL).[32] The non-hydrogen atoms were refined anisotropically, and the hydrogen atoms were calculated using a riding model. CCDC-884226 (**3**·$[Li(TMEDA)_2]_2$) and CCDC-884227 (**3**·$[Li(THF)_4]_2$·3THF) contain the supplementary crystallographical data of this paper. These data can be obtained free of charge at www.ccdc.cam.ac.uk/data_request/cif.

Table 2. Crystal Data and Details of Structural Determination

	3·$[Li(TMEDA)_2]_2$	**3**·$[Li(THF)_4]_2$·3THF
fw	2042.25	1560.80
T [K]	100	100
cryst syst	orthorhombic	monoclinic
space group	*Pnma*	$P2_1$
a [Å]	25.6917(12)	14.949(3)
b [Å]	13.3508(6)	15.745(3)
c [Å]	24.2803(11)	21.602(4)
β [deg]	90	104.93(3)
V [Å^3]	8328.3(7)	4912(2)
Z	4	2
μ [mm^{-1}]	2.8	2.4
δ [g cm^{-3}]	1.63	1.60
radiation source [Å]	0.710 73	0.710 73
Θ-range [deg]	1.58−28.39	1.62−27.95
index range	$-32 \le h \le 34$	$-19 \le h \le 19$
	$-17 \le k \le 16$	$-20 \le k \le 20$
	$-32 \le l \le 32$	$-28 \le l \le 28$
reflns measured	115 683	42 542
indep reflns	10 753	22 650
R(int)	0.0585	0.0560
GOF	1.188	1.078
params/restraints	415/12	805/1
min/max e density [e Å^{-3}]	−1.57/1.97	−0.87/0.78
Flack param		0.007(19)
final R indices $I > 2\sigma$	R1 = 0.0587	R1 = 0.0394
	wR2 = 0.1083	wR2 = 0.0999
final R indices (all data)	R1 = 0.1094	R1 = 0.0425
	wR2 = 0.1307	wR2 = 0.1023
CCDC number	884226	884227

■ ASSOCIATED CONTENT

Ⓢ Supporting Information

Additional figures. Crystallographic data in CIF format. This material is available free of charge via the Internet at http://pubs.acs.org.

■ AUTHOR INFORMATION

Corresponding Author

*E-mail: andreas.schnepf@uni-due.de.

Notes

The authors declare no competing financial interest.

■ ACKNOWLEDGMENTS

This work was financially supported by the Deutsche Forschungsgemeinschaft.

■ DEDICATION

†Dedicated to Professor Jurkschat on the occasion of his 60th birthday.

■ REFERENCES

(1) (a) Sevov, S. C.; Goicoechea, J. M. *Organometallics* **2006**, *25*, 5678−5692. (b) Scharfe, S.; Kraus, F.; Stegmaier, S.; Schier, A.; Fässler, T. F. *Angew. Chem.* **2011**, *123*, 3712−3754;(c) *Angew. Chem., Int. Ed.* **2011**, *50*, 3630−3670. (d) Schnepf, A. *New J. Chem.* **2010**, *34*, 2079−2092.

(2) Schnepf, A. *Angew. Chem.* **2004**, *116*, 680−682; *Angew. Chem., Int. Ed.* **2004**, *43*, 664−666. Schnepf, A. *Chem. Soc. Rev.* **2007**, *36*, 745−758.

(3) Brynda, M.; Herber, R.; Hitchcock, P. B.; Lappert, M. F.; Nowik, I.; Power, P. P.; Protchenko, A. V.; Ruzicka, A.; Steiner, J. *Angew. Chem.* **2006**, *118*, 4439−4443; *Angew. Chem., Int. Ed.* **2006**, *45*, 4333−4337.

(4) Li, F.; Sevov, S. C. *Inorg. Chem.* **2012**, *51*, 2706−2708.

(5) Schnepf, A. *Angew. Chem.* **2003**, *115*, 2728−2729; *Angew. Chem., Int. Ed.* **2003**, *42*, 2624−2625.

(6) Ugrinov, A.; Sevov, S. C. *J. Am. Chem. Soc.* **2002**, *124*, 2442−2443.

(7) Ugrinov, A.; Sevov, S. C. *J. Am. Chem. Soc.* **2003**, *125*, 14059−14064.

(8) Ugrinov, A.; Sevov, S. C. *Chem.—Eur. J.* **2004**, *10*, 3727−3733.

(9) Hull, M. W.; Sevov, S. C. *Angew. Chem.* **2007**, *119*, 6815−6818; *Angew. Chem., Int. Ed.* **2007**, *46*, 6695−6698.

(10) Hull, M. W.; Sevov, S. C. *J. Am. Chem. Soc.* **2009**, *131*, 9026−9037.

(11) Kocak, F. S.; Zavalij, P. Y.; Lam, Y.-F.; Eichhorn, B. W. *Chem. Commun.* **2009**, 4197−4199.

(12) Chapman, D. J.; Sevov, S. C. *Inorg. Chem.* **2008**, *47*, 6009−6013.

(13) Pacher, A.; Schrenk, C.; Schnepf, A. *J. Organomet. Chem.* **2010**, *695*, 941−944.

(14) Schrenk, C.; Köppe, R.; Schellenberg, I.; Pöttgen, R.; Schnepf, A. *Z. Anorg. Allg. Chem.* **2009**, *635*, 1541−1548.

(15) Schrenk, C.; Helmlinger, J.; Schnepf, A. *Z. Anorg. Allg. Chem.* **2012**, *638*, 589−593.

(16) Schrenk, C.; Schellenberg, I.; Pöttgen, R.; Schnepf, A. *Dalton Trans.* **2010**, *39*, 1872−1876.

(17) Besides the influence of the donor applied on the constitution as well as the reactivity of the subhalide, a direct influence of the halide used (SnBr or SnCl) is not obvious.

(18) Additionally, NMR spectroscopic investigations on the crude reaction solution show that the neutral compound $Sn_{10}[Si(SiMe_3)_3]_6$ **1** is not present in the solution.

(19) A 5 mL portion of the reaction solution is dried under reduced pressure, and the resulting black residue is redissolved in THF leading to a dark brown solution. Mass spectra of this THF solution are obtained applying electrospray ionization leading to various signal groups in the mass range between 1500 and 3000 au exhibiting complex isotopic patterns that hint to Sn cluster compounds with a couple of tin atoms.
(20) Due to a possible pseudo-symmetry, space group determination is difficult, and only the cluster core could be localized indicating that a cluster compound with 10 tin atoms within the cluster core is present.
(21) *Holleman–Wiberg Lehrbuch der Anorganischen Chemie*, 102nd ed.; Wiberg, N., Wiberg, E., Holleman, A., Eds.; de Gruyter & Co.: Berlin, 2007.
(22) Fässler, T. F. *Coord. Chem. Rev.* **2001**, *215*, 347.
(23) Quantum-chemical calculations were carried out with the RI-DFT version of the Turbomole program package, by employing the Becke–Perdew 86-functional. The basis sets were of SVP quality. The electronic structure was analyzed with the Ahlrichs–Heinzmann population analysis based on occupation numbers. Turbomole: Treutler, O.; Ahlrichs, R. *J. Chem. Phys.* **1995**, *102*, 346–354. BP-86-functional: Perdew, J. P. *Phys. Rev. B* **1986**, *33*, 8822–8824. Becke, A. D. *Phys. Rev. A* **1988**, *38*, 3098–3100. RI-DFT: Eichkorn, K.; Treutler, O.; Öhm, H.; Häser, M.; Ahlrichs, R. *Chem. Phys. Lett.* **1995**, *240*, 283–290. SVP: Schäfer, A.; Horn, H.; Ahlrichs, R. *J. Chem. Phys.* **1992**, *97*, 2571–2577. Ahlrichs–Heinzmann population analysis: Davidson, E. R. *J. Chem. Phys.* **1967**, *46*, 3320–3324. Roby, K. R. *Mol. Phys.* **1974**, *27*, 81–104. Heinzmann, R.; Ahlrichs, R. *Theor. Chim. Acta* **1976**, *42*, 33–45. Erhardt, C.; Ahlrichs, R. *Theor. Chim. Acta* **1985**, *68*, 231–245.
(24) Wade, K. *Adv. Inorg. Chem. Radiochem.* **1976**, *18*, 1.
(25) A figure of the calculated structure together with all calculated partial charges is given in the Supporting Information Figure S2.
(26) Lippens, P. E. *Phys. Rev. B* **1999**, *60*, 4576–4586.
(27) As HOMO − 3, which is also partly localized at Sn6 (for a picture see Supporting Information Figure S3), exhibits a different symmetry a "transition metal like" chemistry might be possible as lately discussed by Power: Power, P. P. *Nature* **2010**, *463*, 177.
(28) A picture of the evolution of the proton NMR in time is given in Supporting Information Figure S4.
(29) During one attempt to crystallize one of the products of the subsequent reaction we were able to obtain another arrangement of $\{Sn_9[Si(SiMe_3)_3]_2\}^{2-}$ **3** in the solid state where the countercation is now $[Li(THF)_4]^+$ and which crystallizes together with 3 molecules of THF. Nevertheless within **3**·$[Li(THF)_4]_2$·3THF the arrangement of the tin atoms within the cluster core as well as Sn–Sn distances are similar to the one found in **3**·$[Li(TMEDA)_2]_2$. A picture of **3**·$[Li(THF)_4]_2$·3THF is given in the Supporting Information Figure S1.
(30) Schrenk, C.; Neumaier, M.; Schnepf, A. *Inorg. Chem.* **2012**, *51*, 3989–3995.
(31) Fenn, J. B. *Angew. Chem.* **2003**, *115*, 3999–4024; *Angew. Chem., Int. Ed.* **2003**, *42*, 3871–3894.
(32) Sheldrick, G. M. *Acta Crystallogr.* **2008**, *A64*, 112–122.